

# Unusual Interactions Binding Iron Tetrasulfonated Phthalocyanine and Poly(allylamine hydrochloride) in Layer-by-Layer Films

Valtencir Zucolotto,<sup>†</sup> Marystela Ferreira,<sup>†</sup> Márcia R. Cordeiro,<sup>‡</sup> Carlos J. L. Constantino,<sup>§</sup> Débora T. Balogh,<sup>†</sup> Antonio R. Zanatta,<sup>†</sup> Wania C. Moreira,<sup>‡</sup> and Osvaldo N. Oliveira Jr.,<sup>\*,†</sup>

IFSC, USP, CP 369, 13560-970, São Carlos, SP, Brazil, DQ, UFSCar, CP 676, 13565-905, São Carlos, SP, Brazil, and DFQB, FCT, UNESP, CP 467, 19060-900, Presidente Prudente, SP, Brazil

Received: November 27, 2002

Molecular-level interactions are found to bind iron tetrasulfonated phthalocyanine (FeTsPc) and the polyelectrolyte poly(allylamine hydrochloride) (PAH) in electroactive layer-by-layer (LBL) films. These interactions have been identified by comparing Fourier transform infrared (FTIR) and Raman spectroscopy data from bulk samples of FeTsPc and PAH with those from FeTsPc/PAH LBL films. Of particular importance were the  $\text{SO}_3^-$ - $\text{NH}_3^+$  interactions that we believe to bind PAH and FeTsPc and the interactions between unprotonated amine groups of PAH and the coordinating metal of the phthalocyanine. The multilayer formation was monitored via UV-vis spectroscopy by measuring the increase in the Q band of FeTsPc at 676 nm. Film thickness estimated with profilometry was ca. 11 Å per bilayer for films adsorbed on glass. Reflection absorption infrared spectroscopy (RAIRS) revealed an anisotropy in the LBL film adsorbed on gold with FeTsPc molecules oriented perpendicularly to the substrate plane. Cyclic voltammograms showed reproducible pairs of oxidation-reduction peaks at 1.07 and 0.81 V, respectively, for a 50-bilayer PAH/FeTsPc film at 50 mV/s (vs Ag/Ag<sup>+</sup>). The peak shape and current dependence on the scan rate suggest that the process is a diffusion controlled charge transport. In the presence of dopamine, the electroactivity of FeTsPc/PAH LBL films vanishes due to a passivation effect. Dopamine activity is not detected either because the interaction between Fe atoms and  $\text{NH}_2$  groups prevents dopamine molecules from coordinating with the Fe atoms.

## Introduction

Phthalocyanines have been proven suitable materials for photovoltaic, electrochemical, and gas sensing applications.<sup>1,2</sup> Metallic phthalocyanines, in particular, have been exploited as catalysts for a variety of oxidation-reduction reactions<sup>3</sup> and may also be used in neurotransmitters sensors, as they are known to complex with dopamine and serotonin in solution.<sup>4</sup> For example, a complex between dopamine and iron phthalocyanine has been reported,<sup>4</sup> which is attributed to internal electron transfer. Kang et al.<sup>5</sup> used a nickel-phthalocyanine modified electrode as dopamine sensor in electrochemical measurements, where an electrocatalytic effect was observed due to oxidation of dopamine. Because sensing properties of organic materials are usually enhanced when nanostructured films are employed,<sup>6</sup> the fabrication of phthalocyanine ultrathin films has been pursued by a number of groups. Such films are normally prepared with the Langmuir-Blodgett (LB) technique<sup>7</sup> or physical vapor deposition techniques.<sup>8,9</sup> However, recent reports have been made on the fabrication of ultrathin films of metallic phthalocyanines and polyelectrolytes via the electrostatic layer-by-layer technique (LBL).<sup>10–14</sup> In this simple and versatile technique, oppositely charged species can be assembled in a layered structure by ionic interactions between the species in alternated layers.<sup>15,16</sup> In a series of papers,<sup>10–13</sup> Li et al. exploited the LBL films of nickel phthalocyanines as a coating layer onto conducting and semi-

conducting substrates for optical and electronic devices. With the fine control of film thickness and layer architecture, the LBL technique may be used to produce films with tailored properties.

In this work we report the LBL film fabrication of iron tetrasulfonated phthalocyanine (FeTsPc) and poly(allylamine hydrochloride) (PAH). The films comprised molecularly thin layers and displayed electroactivity. Spectroscopic and electrochemical data suggest that unusual interactions occur between the metal coordinating atom of FeTsPc and amine groups from PAH.

## Experimental Details

PAH was purchased from Aldrich and used without further purification. Iron tetrasulfonated phthalocyanine was synthesized according to the method developed by Weber and Busch.<sup>17</sup> Briefly, a solid mixture of 4-sulfophthalic acid, ammonium chloride, urea, ammonium heptamolybdate tetrahydrate, and iron(II) sulfate heptahydrate was added to nitrobenzene at 180 °C. The suspension was heated under stirring at 160–190 °C for 6 h. The solid obtained was then washed and purified. The chemical structures of PAH and FeTsPc are shown in Figure 1. LBL films were assembled onto hydrophilic glass, ITO-coated glass, gold-coated glass, and silicon substrates. The concentration of the dipping solutions was set at 0.3 and 4 mg/mL for PAH and FeTsPc, respectively. The sequential deposition of multilayers was carried out in a HMS series programmable slide stainer (Carl Zeiss Inc) by immersing the substrates alternately into the polycationic and anionic solutions for 5 min. After deposition of each layer, the substrate/film system was rinsed in the washing solution. LBL films were prepared from solutions

\* Corresponding author. Tel: +55-16-273-9825. Fax: +55-16-271-5365. E-mail: chu@ifsc.usp.br.

<sup>†</sup> IFSC.

<sup>‡</sup> DQ.

<sup>§</sup> Unesp.

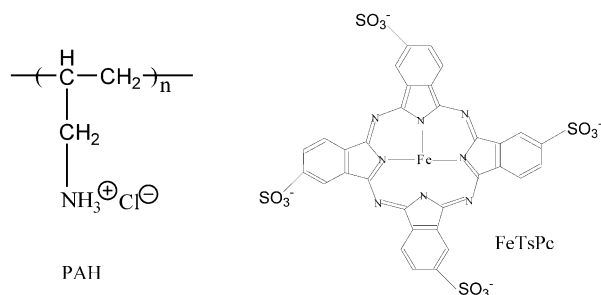


**Figure 1.** Chemical structures of PAH and FeTsPc.

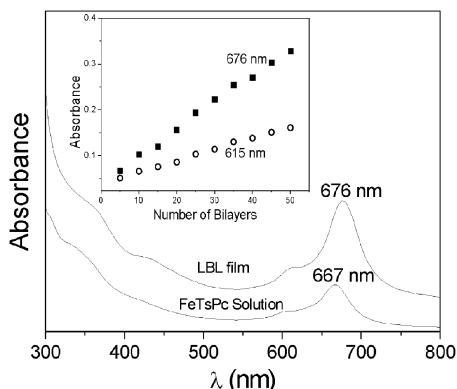


**Figure 2.** Electronic absorption of FeTsPc in aqueous solution and in the LBL film. The inset shows the absorbance at 615 and 676 nm vs number of bilayers for a PAH/FeTsPc film.

with pH = 8. The buildup of the multilayers was monitored at each deposition step by UV-vis spectroscopy. Fourier transform infrared spectroscopy (FTIR) analyses were carried out in a Bomem (Hartmann & Braun), model MB-102 spectrophotometer and the samples were prepared as follows: neat PAH cast film and PAH/FeTsPc LBL films were analyzed onto Si substrates. FeTsPc was analyzed as KBr pellets. Reflection-absorption infrared spectroscopy (RAIRS) for 20-bilayer PAH/FeTsPc LBL film on gold was carried out using a Nicolet Magna-IR 760 spectrometer, DTGS detector, KBr beam splitter,  $4\text{ cm}^{-1}$  spectral resolution, 1000 scans, sample chamber purged with  $\text{N}_2$  gas for 2 h to eliminate water and  $\text{CO}_2$ , and incident angle of  $80^\circ$ . Resonant Raman scattering (Stokes) (RRS) spectra were obtained with a Renishaw Research Raman Microscope System RM2000. The RM2000 uses a Leica microscope (DMLM series) and a  $50\times$ -microscope objective to focus the laser beam onto a spot of ca.  $1.0\text{ }\mu\text{m}^2$ . The spectra were taken using a 633 nm laser line from a He-Ne Laser. They are recorded using a Peltier cooled ( $-70^\circ\text{C}$ ) CCD array with ca.  $4\text{ cm}^{-1}$  spectral resolution, at room temperature. Cyclic voltammetry was carried out using an Autolab PGSTAT30, at room temperature and with various scan rates (20, 50, 100, and 200 mV/s). The counter electrode was a platinum sheet with an area of  $1.5\text{ cm}^2$ . The quasi-reference electrode was an  $\text{Ag}/\text{Ag}^+$  wire. ITO conducting glass with an area of  $1\text{ cm}^2$  served as working electrode. An electrolytic solution of 0.1 M  $\text{LiClO}_4$  (Aldrich) in acetonitrile (Aldrich) was used in all electrochemical experiments.

## Results and Discussion

**Film Growth and Electronic Absorption of PAH/FeTsPc LBL Films.** Figure 2 displays the UV-vis spectra for a 55-bilayer PAH/FeTsPc LBL film and for an FeTsPc aqueous solution. The absorbance is entirely due to FeTsPc because PAH does not absorb in this region. The peak at 676 nm (Q-band of

the phthalocyanine) corresponds to the electronic absorption of FeTsPc monomeric species whereas the shoulder at 615 nm corresponds to the electronic absorption of dimeric species of FeTsPc<sup>18–20</sup> (bridged by  $\text{O}_2$  molecules). A small shift in the absorbance of the Q-band was observed between the spectra of FeTsPc in aqueous solution and in the LBL films. Two possible reasons may be suggested to explain the red shift in the film: (1)  $\pi$ -stacking of FeTsPc molecules in a face-to-face conformation. Indeed, the relative intensity between the monomeric and dimeric Q-bands ( $A_{676\text{nm}}/A_{615\text{nm}}$ ) in the film is smaller than that in the solution, suggesting the presence of more dimeric species in the films, and (2) interaction between the nonprotonated  $\text{NH}_2$  groups from PAH and the coordinating metal of the phthalocyanine. This hypothesis is supported by FTIR measurements to be discussed later. The inset in Figure 2 shows that the absorbance at 615 and 676 nm increases linearly with the number of layers; i.e., the amount of adsorbed FeTsPc is the same in each deposition cycle. The average thickness of the multilayers was determined by profilometry to be ca.  $11\text{ }\text{\AA}$  per bilayer for a 55-bilayer PAH/FeTsPc film adsorbed on glass. Li et al.<sup>11</sup> observed a mean thickness of  $10.5\text{ }\text{\AA}$  per bilayer for LBL films of poly(diallyldimethylammonium) chloride (PDAC) and nickel tetrasulfonated phthalocyanine (NiTsPc) deposited on silica. Lütt et al. also reported a thickness of  $10\text{ }\text{\AA}$  for PDAC/NiTsPc bilayers deposited on silica. In the latter, however, the authors found a thickness value of ca.  $20\text{ }\text{\AA}$  for the first few bilayers of PDAC/NiTsPc deposited on silicon substrates. A possible explanation for such thick bilayers formed on Si was that PDAC and NiTsPc adsorbed in a standing up arrangement. In the present work, specifically for the PAH/FeTsPc films deposited on glass substrates, however, it was not possible to infer about the orientation of FeTsPc molecules. Because some degree of interpenetration between the adjacent layers of PAH and FeTsPc are expected,<sup>15</sup> the thickness values are inconclusive in terms of FeTsPc molecule configuration. On the other hand, on the basis of vibrational spectroscopy analysis, it was possible to determine that for the PAH/FeTsPc films deposited on gold-coated substrates, the FeTsPc molecules adopt a standing up conformation even if interpenetration occurs, as will be discussed in the next section.

**Vibrational Spectroscopic Characterization of the LBL Films.** The interactions between the iron phthalocyanine and PAH in the LBL films were investigated with FTIR measurements, which were carried out on neat PAH (cast film onto Si), neat FeTsPc (in KBr pellets), and a 50-bilayer PAH/FeTsPc LBL film deposited onto a Si substrate. The spectra are shown in Figure 3. The main bands of PAH are assigned with wavenumbers in  $\text{cm}^{-1}$  as 1576 (N–H bending) and 1383 and 1335 (C–H bending). FeTsPc-KBr pellets displayed the main absorption bands: 769 (ring breathing, C–H wagging), 994 (Fe–Pc), 1042 ( $\text{SO}_3$  stretch), 1134 (C–H bending), 1199 ( $\text{SO}_3$  stretch), 1406 and 1489 (isoindole stretch), 1630 ( $\text{C}=\text{C}$  benzene stretch). The band at  $1720\text{ cm}^{-1}$  was assigned to the carbonyl stretch of a sulfophthalic acid molecule as axial ligand coordinated to the metal ion (M-axial ligand). The band at  $1042\text{ cm}^{-1}$  due to the  $\text{SO}_3$  stretch in spectrum b appears as a stronger band shifted to  $1025\text{ cm}^{-1}$  in the PAH/FeTsPc film spectrum c. In addition, the band at  $1199\text{ cm}^{-1}$  ( $\text{SO}_3$  stretch) splits into two bands at 1177 and  $1224\text{ cm}^{-1}$  with an increase in relative intensity in the LBL film compared to the neat FeTsPc pellet. These changes occurred due to the formation of salt bridges of  $\text{SO}_3^-$ - $\text{NH}_3^+$ , which act as binding forces between PAH and FeTsPc in the LBL films.<sup>12,13</sup> The band at  $1720\text{ cm}^{-1}$  assigned to the metal-axial ligand of FeTsPc is very strong in the FeTsPc

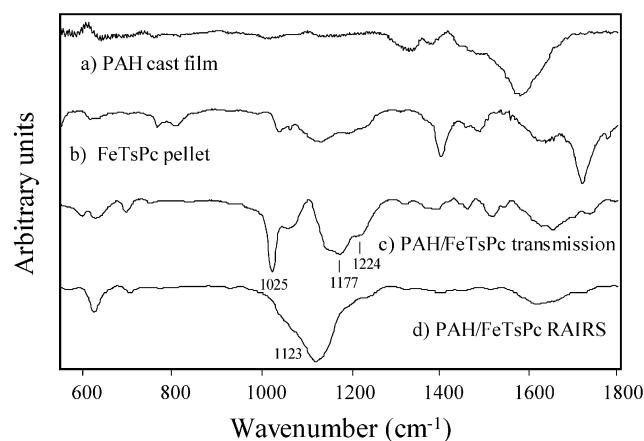


**Figure 3.** FTIR spectra for neat PAH and FeTsPc and for LBL films of PAH/FeTsPc onto Si (50 bilayers, transmission mode) and onto Au (20 bilayers, RAIRS mode).

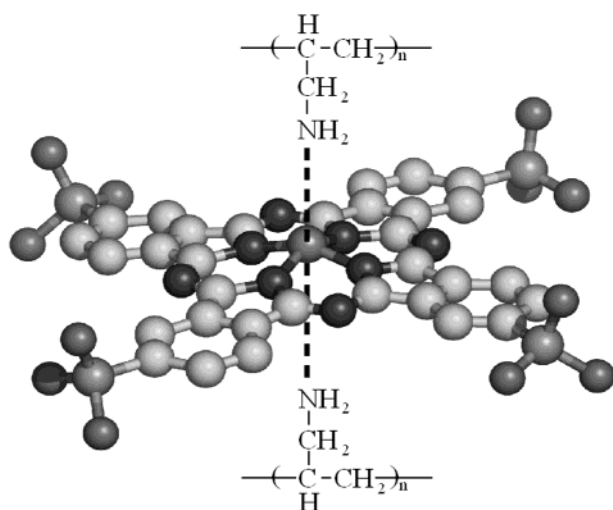


**Figure 4.** Suggested additional interaction binding the Fe atom and unprotonated  $\text{NH}_2$  groups from PAH.

KBr pellet but has its relative intensity drastically decreased in the PAH/FeTsPc LBL film. Furthermore, the isoindole and pyrrole stretch and the Pc breathing vibrations also shift in the IR spectrum of the PAH/FeTsPc LBL film, which may be associated with changes in the electronic environment in the metallic center of the macrocycle ring. These results indicate that, besides the expected salt bridges between the sulfonic and protonated amino groups, there is an additional and unusual interaction between the phthalocyanine molecule, through its metallic center, and the PAH in the LBL film, as illustrated in Figure 4. As the structure of PAH contains a hydrocarbon main chain, only the nitrogen atom of the amino group could act as a possible ligand to the metallic atom, if the amino group is unprotonated. The  $\text{p}K_{\text{a}}$  of amino groups is approximately 9.7,<sup>21</sup> thus at  $\text{pH} = 8$  the concentration of protonated  $\text{NH}_2$  groups is estimated to be 50 times the concentration of unprotonated groups. Nevertheless, unprotonated groups will still be available to coordinate axially with iron at FeTsPc.

Complementarily, RAIRS was carried out for a 20-bilayer PAH/FeTsPc LBL film deposited onto Au (spectrum d in Figure 3) to investigate possible anisotropy in the film. The analysis consider the surface selection rules<sup>22</sup> and the key bands of Pc such as 1123 and 1066  $\text{cm}^{-1}$  assigned to in-plane C—H bending and the bands within the range 700–800  $\text{cm}^{-1}$  assigned to out-of-plane C—H wagging.<sup>9</sup> Figure 3 shows that the band at ca. 1123  $\text{cm}^{-1}$  dominates the RAIRS spectrum for the LBL film

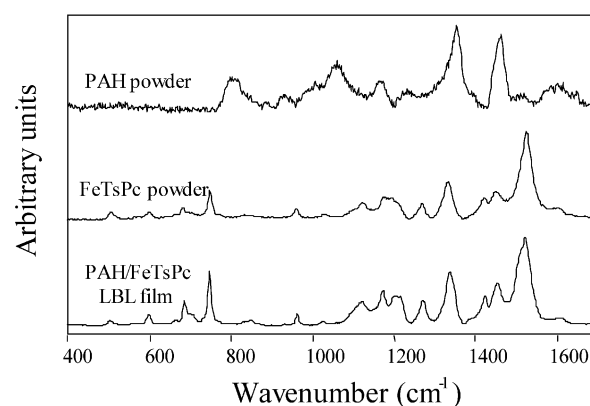


**Figure 5.** Raman scattering spectra recorded with the 633 nm laser line for PAH and FeTsPc (powder) and for a 55-bilayer LBL film of PAH/FeTsPc.

whereas it vanishes in the transmission mode. According to the surface selection rules, the incident electric field lies on the substrate plane for the transmission mode (normal incidence of the light) and the p-component of the incident electric field, which is perpendicular to the substrate plane, is maximized in relation to the s-component by the experimental conditions. Besides, the surface selection rules predict that the induced dipole moments oriented preferentially perpendicular to the substrate plane will be stronger in the RAIRS mode whereas those that are preferentially parallel to the plane substrate will be stronger in the transmission mode. Therefore, considering the key bands of Pc used here, one concludes that the FeTsPc molecules are perpendicular to the substrate plane. It must be noted that the C—H bending modes from PAH do not play an important role here because they are not well-defined in terms of signal/noise ratio even for the pure PAH cast film whose concentration is much higher than that used during the PAH/FeTsPc LBL film fabrication. The broadening of the 1123  $\text{cm}^{-1}$  could be related to the overlapping of the in-plane C—H bending and other bands such as those from the  $\text{SO}_3$  groups.

Raman scattering data, shown in Figure 5 for PAH and FeTsPc (powders) and for PAH/FeTsPc LBL films onto hydrophilic glass, confirmed the observations obtained from the FTIR spectra. Table 2 summarizes the assignments for the Raman bands. The differences in the LBL film are not as clear as in the FTIR spectra, but one may note that a new band at 1217  $\text{cm}^{-1}$  arises in the LBL film. This band is attributed to a  $\text{SO}_3^-$ - $\text{NH}_3$  bridge between PAH and FeTsPc, consistent with the FTIR analysis. Also, minor changes can be observed at the isoindole and pyrrole stretch region, mainly a small shift and the shoulder at 1504  $\text{cm}^{-1}$  in the PAH/FeTsPc LBL film. Such changes may be related to the additional interaction between the metal ion of FeTsPc and amine moieties in the PAH structure.

**Cyclic Voltammetry.** Figure 6 depicts the cyclic voltammograms for a PAH/FeTsPc 50-bilayer LBL film deposited onto ITO, obtained in 0.1 M  $\text{LiClO}_4$  in acetonitrile at different scan rates. When the potential was scanned between 0.4 and 1.4 V, a redox wave was observed with the redox potential at 1.07 and 0.81 V, respectively. The redox mechanism is attributed to  $\text{Fe}^{2+}/\text{Fe}^{3+}$  processes. When the scan rate is increased, the potentials of the anodic and cathodic peaks shift symmetrically, resulting in a constant formal potential at various scan rates. As shown in the inset of Figure 6, the anodic peak current ( $I_{\text{pa}}$ ) varies linearly with the square root of the scan rate, which indicates that the peak current is diffusion controlled, in agreement with Lvov's report.<sup>14</sup> In their work on LBL films of phthalocyanines, they observed that the voltammetric behavior



**TABLE 1: Peak Assignment for the FTIR Data for PAH and FeTsPc Powder and for a 50-Bilayer PAH/FeTsPc LBL Film**

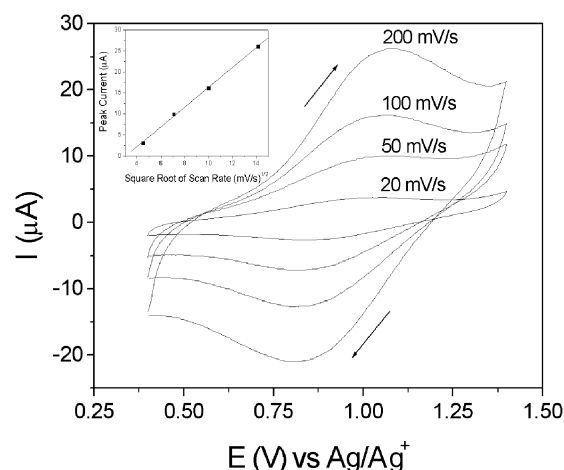
assignment	PAH powder	FeTsPc powder	LBL 50-bilayer PAH/FeTsPc
macrocycle vibration			600
macrocycle vibration		621	
macrocycle vibration			632
			698
Pc breathing		769	
macrocycle vibration		809	
Fe—Pc		994	
SO <sub>3</sub> stretch			1025
SO <sub>3</sub> stretch		1042	
SO <sub>3</sub> stretch		1065	1063
C—H bending		1134	
			1177
SO <sub>3</sub> stretch		1199	1224
C—H bending			
Pyrrole stretch			1326
C—H Bending	1335		
C—H deformation			1346
C—H bending	1383		
isoindole stretch		1406	
isoindole stretch			1464
isoindole stretch		1489	
C=C, C=N pyrrole stretch			1517
			1548
N—H bending	1576		
benzene stretch		1630	1625
			1655
Fe—axial ligand		1720	
			1730

**TABLE 2: Assignment of Raman Bands for PAH and FeTsPc Powder and for a 55-Bilayer PAH/FeTsPc LBL Film**

assignment	PAH powder	FeTsPc powder	LBL 55-bilayer PAH/FeTsPc
isoindole deformation		508	506
macrocycle vibration		601	600
macrocycle vibration		680	688
macrocycle vibration		749	748
	809		
			846
	930		
benzene breathing		962	962
C—H bending		1030	1023
C—H bending	1061		
C—H bending		1121	1119
C—H bending	1166		
		1174	1171
SO <sub>3</sub> stretch		1196	1200
			1213
C—H bending		1269	1269
pyrrole stretch		1331	1336
C—H deformation	1353		
isoindole stretch		1418	1421
isoindole stretch		1447	1450
C—N stretch	1461		
			1504 sh
C=C, C=N pyrrole stretch		1525	1520
	1583		
benzene stretch	1600	1600	1600

of cobalt phthalocyanine LBL films was controlled by charge transport.<sup>23</sup> Subsidiary experiments of cyclic voltammetry were carried out in situ with red light irradiation,  $\lambda = 660$  nm. The absorbance changed by only 3% as the applied potential was varied, thus indicating that PAH/FeTsPc LBL films do not have their color changed significantly during the anodic/cathodic voltammetric process.

The electrochemical catalytic effect of phthalocyanine-modified electrodes for detecting dopamine (DA) is well-

**Figure 6.** Cyclic voltammograms for a 50-bilayer LBL film in 0.1 M LiClO<sub>4</sub> in acetonitrile at different scan rates (20, 50, 100, and 200 mV/s). The inset shows the dependence of the anodic peak current on the square root of the scan rate.

known.<sup>5</sup> In ref 5 it was shown that the oxidation current at the anodic peak potential for dopamine was approximately 3 times that for the nickel phthalocyanine—carbon glass (GC) modified electrodes in comparison to bare GC electrodes. The catalytic effect of FeTsPc for dopamine, in particular, has been probed in our group with ITO-coated glass substrates modified with LBL films from polyaniline (PANI) alternated with FeTsPc.<sup>24</sup> The electrochemical response for PANI/FeTsPc-modified electrodes showed an additional well-defined pair of oxidation–reduction peaks at 0.207 and 0.02 V (vs Ag/Ag<sup>+</sup>), respectively, with the addition of 5 mM of dopamine in the electrolyte solution. Electrodes modified with PANI without FeTsPc (using an electrochemically inert anionic polyelectrolyte to assemble the films) displayed only an additional reduction peak at −0.05 V in the presence of dopamine. It is also well established that dopamine and FeTsPc can form a [(DA<sup>+</sup>)FeTsPc]<sup>4+</sup> complex via internal electron transfer in solution,<sup>4</sup> which requires the coordination of both oxygen atoms from dopamine with the metal of phthalocyanine. One should therefore expect some degree of interaction between DA and FeTsPc in the solid state, as it occurs for NiTsPc and PANI/FeTsPc-modified electrodes (as discussed above). On the other hand, in the PAH/FeTsPc LBL films, the interactions between Fe and NH<sub>2</sub> groups of PAH could prevent the dopamine oxygen atoms from approaching the metal atom, which eliminates the electroactivity of dopamine.

To check any catalytic effect in the films, we subjected the PAH/FeTsPc LBL films for detecting dopamine via cyclic voltammetry. The measurements were taken under the same conditions described for Figure 6. Figure 7 shows the voltammograms with a scan rate of 50 mV/s<sup>−</sup> of the LBL film in the electrolytic solution (curve a), in the presence of dopamine at  $9 \times 10^{-5}$  M (curve b), and in the absence of dopamine after the LBL film-coated electrode had been thoroughly washed in acetonitrile. With dopamine in the solution, there is almost complete extinction of the oxi-reduction peaks (curve b), but this effect is reversible. After the electrodes are washed, the electroactivity of the films is recovered (curve c). The same effect was observed for other concentrations of dopamine. Two important features can be drawn from these experiments. First, the electrode passivation in curve b is probably due to the adsorption of DA molecules onto the substrate. Such a DA layer effectively contributes to a fouling effect of the electrode, which leads to extinction of the oxi-reduction peaks from FeTsPc

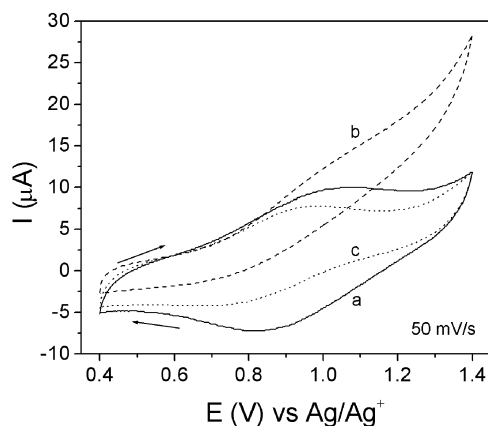


**Figure 7.** Cyclic voltammograms from a 50-bilayer PAH/FeTsPc film as deposited (a), in the presence of dopamine (b), and after washing with acetonitrile (c).

shown in Figure 6. Second, as DA is known to be electroactive,<sup>5</sup> oxi-reduction peaks should have been observed. Therefore, the absence of peaks in the voltammograms must have been caused by interactions between the coordinating metal and  $\text{NH}_2$ , which hindered any DA-Fe atom approach, consistent with the earlier discussion of the FTIR data.

## Conclusions

Electroactive layered films of iron phthalocyanine were obtained via the LBL technique. Vibrational analyses showed strong  $\text{SO}_3^-$ - $\text{NH}_3^+$  salt bridges acting as binding forces between FeTsPc and PAH. There was also evidence for an unusual interaction between the coordinating metal of FeTsPc and the unprotonated  $\text{NH}_2$  groups of PAH. Such interactions are believed to be associated with the nanostructured nature of the LBL films, which provide intimate contact between the film components. To our knowledge this is the only work in which interactions have been reported involving coordinating metals for phthalocyanines in LBL films. The molecular orientation in the LBL film was determined by combining transmission and reflection modes in the infrared absorption. The Pc molecules are oriented perpendicular to the substrate surface for a gold substrate. The PAH/FeTsPc LBL films displayed electroactivity with oxi-reduction peaks from FeTsPc centered at 1.07 and 0.81 V. The electroactivity of PAH/FeTsPc LBL films vanished in the presence of dopamine, as the latter molecules caused a passivation effect. The electroactivity of dopamine could not be detected either, as the interaction between Fe atoms and  $\text{NH}_2$

groups had the screening effect of impairing dopamine to axially coordinate with the Fe atom. Because the interactions in the LBL film may be controlled by changing the pH of the solutions to prepare the films, the interplay between such interactions can be exploited in sensing dopamine.

**Acknowledgment.** We are grateful to FAPESP and CNPq for the financial support and to Dr. Teodosio del Cano, University of Valladolid, Spain, for the RARS analysis.

## References and Notes

- (1) Peumans, P.; Forrest, S. R. *Appl Phys Lett* **2002**, *80*, 338.
- (2) Pontie, M.; Gobin, C.; Pauporte, T.; Bediou, F.; Devynck, J. *Anal. Chim. Acta* **2000**, *411*, 175.
- (3) Vilakazi, S. L.; Nyokong, T. *Polyhedron* **1998**, *17*, 4415.
- (4) Oni, J.; Nyokong, T. *Polyhedron* **2000**, *19*, 1355.
- (5) Kang, T.-F.; Shen, L.-G.; Yu, R.-Q. *Anal. Chim. Acta* **1997**, *356*, 245.
- (6) Wossmeier, T.; Guse, B.; Besnard, I.; Bauer, R. E.; Müllen, K.; Yasuda, A. *Adv. Mater.* **2002**, *14*, 238.
- (7) Gaffo, L.; Constantino, C. J. L.; Moreira, W. C.; Aroca, R. F.; Oliveira, O. N., Jr. *Langmuir* **2002**, *18*, 3561.
- (8) Ho K.-C.; Tsou, Y.-H. *Sens. Actuators B* **2001**, *77*, 253.
- (9) Aroca, R.; Thedchanamoorthy, A. *Chem. Mater.* **1995**, *7*, 69.
- (10) Lütt, M.; Fitzsimmons, M. R.; Li, D. Q. *J. Phys. Chem. B* **1998**, *102*, 400.
- (11) Li, D. Q.; Lutt, M.; Fitzsimmons, M. R.; Synowicki, R.; Hawley, M. E.; Brown, G. W. *J. Am. Chem. Soc.* **1998**, *120*, 8797.
- (12) Li, L. S.; Wang, R.; Fitzsimmons, M.; Li, D. Q. *J. Phys. Chem. B* **2000**, *104*, 11195.
- (13) Li, L. S.; Jia, Q. X.; Li, A. D. Q. *Chem. Mater.* **2002**, *14*, 1159.
- (14) Lvov, Y. M.; Kamau, G. N.; Zhou, D.-L.; Rusling, J. F. *J. Colloid Interface Sci.* **1999**, *212*, 570.
- (15) Oliveira, O. N., Jr.; He, J.-A.; Zucolotto, V.; Balasubramanian, S.; Li, L.; Nalwa, H. S.; Kumar, J.; Tripathy, S. K. *Layer-by-Layer Polyelectrolyte Films for Electronic and Photonic Applications*. In *Handbook of Polyelectrolytes and Their Applications, Vol. 1*; Kumar, J., Nalwa, H. S., Eds.; American Scientific Publishers: Los Angeles, 2002; pp 1–37.
- (16) Decher, G.; Hong, J. D.; Schmitt, J. *Thin Solid Films* **1992**, *210/211*, 831.
- (17) Weber, J. H.; Busch, D. H. *Inorg. Chem.* **1965**, *4*, 469.
- (18) Guo, L.; Ma, G.; Liu, Y.; Mi, J.; Qian S.; Qiu, L. *Appl. Phys. B* **2002**, *74*, 253.
- (19) Smith, W. E.; Rospendowski, B. N. *Raman Spectra of Phthalocyanines*. In *Phthalocyanines: Properties and Applications, Vol. 3*; Leznoff, C. C., Lever, A. B. P., Eds.; VCH Publishers: New York, 1993; pp 167–225.
- (20) Kasuga, K.; Tsutsui, M. *Coord. Chem. Rev.* **1980**, *32*, 67.
- (21) Tsukruk, V. V.; Rinderspacher, F.; Bliznyuk, V. N. *Langmuir* **1997**, *13*, 2171.
- (22) Antunes, P. A.; Constantino, C. J. L.; Duff, J.; Aroca, R. *Appl. Spectrosc.* **2001**, *55*, 1341 and references therein.
- (23) Murray, L. W., Ed. *Molecular Design of Electrode Surfaces*; Techniques of Chemistry, Vol. 22; Wiley: New York, 1992.
- (24) Zucolotto, V.; Ferreira, M.; Cordeiro, M. R.; Constantino, C. J. L.; Balogh, D. T.; Moreira, W. C.; Oliveira, O. N., Jr. Unpublished results.